Supporting Information

An Easily Available Ratiometric Reaction-based AIE Probe for Carbon Monoxide Light-up Imaging

Jianguo Wang,[†,‡,#] Chunbin Li,[‡,§,#] Qingqing Chen,[‡] Hongfeng Li,[§] Lihua Zhou,[§] Xing Jiang,[§] Mengxue Shi,[‡] Pengfei Zhang,[§,*] Guoyu Jiang[†,‡,*] and Ben Zhong Tang[⊥,*]

†College of Chemistry and Chemical Engineering, Inner Mongolia Key Laboratory of Fine Organic Synthesis, Inner Mongolia University, Hohhot 010021, China. * E-mail: jiangguoyu@mail.ipc.ac.cn

‡Key Laboratory of Organo-Pharmaceutical Chemistry, Gannan Normal University, Ganzhou 341000, China.

§Guangdong Key Laboratory of Nanomedicine, CAS Key Laboratory of Health Informatics, Shenzhen Bioactive Materials Engineering Lab for Medicine, Institute of Biomedicine and Biotechnology, Shenzhen Institutes of Advanced Technology, Chinese Academy of Sciences, Shenzhen 518055, China. * E-mail: pf.zhang@siat.ac.cn

⊥Department of Chemistry, Hong Kong Branch of Chinese National Engineering Research Center for Tissue Restoration and Reconstruction, Institute for Advanced Study, Division of Biomedical Engineering, Division of Life Science, State Key Laboratory of Molecular Neuroscience and Institute of Molecular Functional Materials, The Hong Kong University of Science and Technology (HKUST), Clear Water Bay, Kowloon, China. HKUST Shenzhen Research Institute, No. 9 Yuexing 1st RD, South Area Hi-tech Park, Nanshan, Shenzhen 518057, China.

* E-mail: tangbenz@ust.hk

[#]These authors contributed equally to this work.

Table of Contents

Experiment section:

Figures and tables:

Experiment section:

Materials and instrumentation

Chemicals were purchased from Energy-Chemical, Sigma-Aldrich, J&K and used without further purification. Solvents and other common reagents were obtained from Sigma-Aldrich. ^{1}H NMR and ^{13}C NMR spectra were measured on a Bruker ARX 400 MHz spectrometer. High-resolution mass spectra (HRMS) were recorded on a GCT Premier CAB 048 mass spectrometer operating in MALDI-TOF mode. UV-vis absorption spectra were recorded on a Rarian 50 Conc UV-Visible spectrophotometer. Fluorescence emission spectra were recorded on a Edinburgh FS5 fluorescence spectrophotometer. Absolute fluorescence quantum yield were measured on Hamamatsu C11347-11 Quantaurus-QY Absolute PL quantum yield spectrometer. Cellular imaging experiments were performed with confocal laser scanning microscope (TCS SP5, Leica, Germany) equipped with Argon, red HeNe, and green HeNe lasers.

General procedures for the detection of CO

Unless otherwise noted, all the spectral measurements were performed in 5 mM phosphate buffer (pH 7.4, containing 5% DMSO) according to the following procedure. The stock solution (1.0 mM) of probe BTCV-CO was first prepared in DMSO. 10 μL of BTCV-CO stock solution was added to 2 mL PBS followed by addition of different volume of CO solution. The mixture was incubated for certain times at 37 ^{o}C and then, the reaction solution was transferred to a quartz cell with 1 cm optical length for measurements. In the meantime, the blank solution without CO was also prepared and measured under the same conditions for comparison.

CO was prepared from $[Ru(CO)_3Cl_2]_2$ (CORM-2) in aqueous solution. Hydrogen peroxide (H_2O_2) and hypochlorite (ClO^-) were delivered from 30% and 5% aqueous solutions, respectively. Hydroxyl radical (•OH) was generated by reaction of 100 μM Fe^{2+} with 100 μM H_2O_2. ROO• was generated from 2,2'-azobis(2-amidinopropane)dihydrochloride (AAPH), which was dissolved in deionizer water and then stirred at 25 ^{o}C for 30 min. Theoretically, 1 equiv of AAPH will generate 2 equiv of ROO•. R stands for 2-amidinoisopropyl. $ONOO^-$ was prepared according to the literature and modified.[S1] A mixture of 50 mM sodium nitrite and 50 mM hydrogen peroxide in 50 mL of ice-cold water was rapidly stirred in a 250 mL beaker. A solution of hydrochloric acid (1 M, 25 mL) is rapidly thrown into the nitrite/peroxide solution followed by a solution of sodium hydroxide (1.5

M, 25 mL) approximately 1 second later. The concentration of $ONOO^-$ was determined by UV spectrophotometry (ε_{302} = 1670 L • mol^{-1} • cm^{-1}). Angeli's salt (AS) was purchased from Santa Cruz Biotechnology, and HNO was prepared from AS using double-distilled water.

Determination of CO concentration released from CORM-2

The release of CO from CORM-2 was assessed spectrophotometrically by measuring the conversion of deoxymyoglobin (deoxy-Mb) to carbonmonoxy myoglobin (MbCO). The amount of MbCO formed was quantified by measuring the absorbance at 540 nm (extinction coefficient=15.4 $mmol \cdot L^{-1} \cdot cm^{-1}$). Myoglobin solutions (66 μmol/L final concentration) were prepared fresh by dissolving the protein in 0.04 mol/L phosphate buffer (pH=6.8). Sodium dithionite (0.1%) was added to convert myoglobin to deoxy-Mb. CO released from CORM-2 was quantified by adding aliquots of stock solutions (10 μL) of CORM-2 in DMSO directly to the myoglobin solution.

Determination of the detection limit of BTCV-CO toward addition of CO

Based on the linear fitting in Figure 2C and Figure S14, the detection limit (C) is estimated as follows:

$$C = 3\sigma/B \qquad (1)$$

Where σ is the standard deviation obtained from three individual fluorescent intensity ratio (I_{546}/I_{710}) or ($(I-I_0)/I_0$) at 546 nm of BTCV-CO (5 μM) without any CO and B is the slope obtained after linear fitting the titration curves within certain ranges.

Cell cultures

The MCF-7 cells were cultured in DMEM (containing 10% heat-inactivated FBS, 100 $mg \cdot mL^{-1}$ penicillin and 100 $mg \cdot mL^{-1}$ streptomycin) at 37 °C in a humidified incubator with 5% CO_2. Before the experiments, the cells were pre-cultured until confluence was reached.

Cell viability

Cell viability was determined by using MTT assay which is based on the reduction of 3-(4,5-dimethythiazol-2-yl)-2,5-diphenyl tetrazolium bromide (MTT, yellow in color) into formazan (blue color) by mitochondrial succinate dehydrogenase. Dispense 100 μL of cell suspension (5000 cells/well) in a 96-well plate. Pre-incubate the plate for 24 h at 37 °C in a humidified incubator with 5% CO_2. Add 10 μL of various concentrations of BTCV-CO into the culture media in the plate. After incubating the plate for 24 h in the incubator, the cell medium were

exchanged with fresh medium (100 μL), and then 20 μL of the MTT (5 mg/mL) solution was then added. Medium was removed after the incubation period of 4 hours followed by the addition of 100 μL of DMSO to dissolve the formazan crystals. Absorbance was taken at 600 nm by an ELISA Plate Reader (Biotek Synergy HT). Untreated cells were taken as control. All the experiments were performed in triplicate. Cell viability was determined by using given formula:

$$\text{Cell viability (\%)} = \frac{\text{Absorbance of treated cells}}{\text{Absorbance of untreated cells}} \qquad (2)$$

Cell treatment and cell imaging

For the imaging of CO, the MCF-7 cells were incubated with 5 μM BTCV-CO and 5 μM $PdCl_2$ for 30 min at 37 °C, then the media was replaced with PBS buffer and the cells were treated with different concentrations of CORM-2 (0, 10, 20 and 50 μM) for 30 min. The imaging was acquired using a confocal laser scanning microscope (TCS SP5, Leica, Germany). For cell imaging, the cells were washed with PBS three times. A 476 nm laser was used as the light source and emission was collected from 500 to 580 nm (green channel) and 580 to 700 nm (red channel).

***In vivo* animal imaging**

Female BALB/c white mice (4–6 weeks old and weighted 25–30 g) were purchased from Vital River Laboratory Animal Technology Co. Ltd (Beijing, China) and all animals received care incompliance with the guidelines outlined in the Guide for the Care and Use of Laboratory Animals. The procedures were approved by Shenzhen Institutes of Advanced Technology, Chinese Academy of Sciences Animal Care and Use Committee. The probe solution (25 μL, 1 mM in DMSO) was injected to white mice *via* intraperitoneal injection, followed by an injection of CORM-2 (75 μL, 2 mM). Control group was injected with 75 μL of PBS. Images were taken after injection using the Maestro *in vivo* imaging system.

Scheme S1. Synthetic route to BTIC.

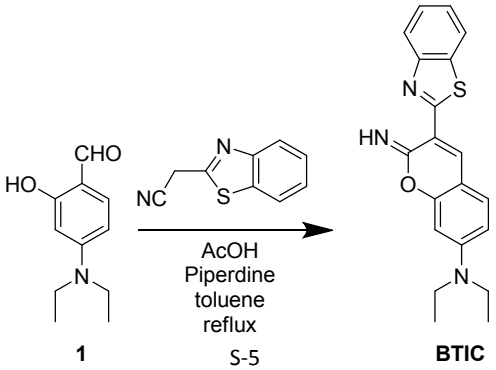

Synthesis of compound 3. 4-(Diethylamino)salicylaldehyde (compound **1**, 193.0 mg, 1.0 mmol), allyl bromide (compound **2**, 242.0 mg, 2.0 mmol) and K_2CO_3 (415.0 mg, 3.0 mmol) was mixed in 10 mL CH_3CN. The mixture was refluxed under the nitrogen atmosphere. The reaction was monitored by TLC. When compound **1** disappeared, the mixture was cooled to room temperature and filtrated to remove any solids. The obtained solution was washed with brine and extracted with dichloromethane. The organic layer was dried over anhydrous Na_2SO_4. After concentrated, the residue was purified by silica gel chromatography with petroleum ether/dichloromethane (1:2～2:1, *v*/*v*) to give compound **3** as a white solid (212.0 mg, 91%). ^{1}H NMR (400 MHz, $CDCl_3$) δ 10.09 (s, 1H), 7.59 (d, J = 8.9 Hz, 1H), 6.16 (d, J = 10.4 Hz, 1H), 5.94 (d, J = 2.0 Hz, 2H), 5.35 (d, J = 18.3 Hz, 1H), 5.21 (d, J = 10.6 Hz, 1H), 4.52 (d, J = 5.0 Hz, 2H), 3.32-3.27(m, 4H), 1.17-1.08 (m, 6H). ^{13}C NMR (100 MHz, $CDCl_3$) δ 186.77, 163.21, 153.79, 132.97, 130.18, 117.35, 114.18, 104.41, 93.67, 68.78, 44.74, 12.52.

Synthesis of BTCV-CO. A mixture of compound **3** (117.1 mg, 0.5 mmol), benzothiazole-2-yl-acetonitrile (174.2 mg, 1.0 mmol), piperidine (150 μL, 1.6 mmol), acetic acid (150 μL, 2.6 mmol) in 25 mL toluene was refluxed under nitrogen atmosphere for 16 h. After cooling to room temperature, the mixture was washed with brine and extracted with dichloromethane. The organic layer was dried over anhydrous Na_2SO_4. After concentrated, ethyl ether/dichloromethane (15:1, *v*/*v*) was added and BTCV-CO was precipitated and collected as a red solid (166.1 mg, 85%). ^{1}H NMR (400 MHz, $CDCl_3$) δ 8.57 (s, 1H), 8.43 (d, J = 9.2 Hz, 1H), 8.01 (d, J = 8.1 Hz, 1H), 7.83 (d, J = 7.9 Hz, 1H), 7.49 – 7.41 (m, 1H), 7.38 – 7.30 (m, 1H), 6.37 (m, 1H), 6.20 – 6.03 (m, 2H), 5.50 (d, J = 18.8 Hz, 1H), 5.37 (d, J = 11.9 Hz, 1H), 4.67-4.65 (m, 2H), 3.45-3.40 (m, 4H), 1.24-1.21 (m, 6H). ^{13}C NMR (100 MHz, $CDCl_3$) δ 165.91, 160.46, 153.99, 152.58, 141.21, 134.42, 133.01, 130.53, 126.32, 124.85, 122.90, 121.26, 118.63, 117.65, 110.04, 105.25, 96.42, 94.36, 69.28, 44.90, 12.72. HRMS (MALDI-TOF): *m*/*z*: $[M]^+$ calcd for $C_{23}H_{23}N_3OS^+$: 389.1562; found: 389.1602.

Synthesis of BTIC. A mixture of compound **1** (97.1 mg, 0.5 mmol), benzothiazole-2-yl-acetonitrile (174.3 mg, 1.0 mmol) piperidine (150 μL, 1.6 mmol), acetic acid (150 μL, 2.6 mmol) in 25 mL toluene was refluxed under nitrogen atmosphere for 16 h. After cooling to room temperature, the mixture was washed with brine and extracted with dichloromethane. The organic layer was dried over anhydrous Na_2SO_4. After concentrated, ethyl ether/dichloromethane (30:1, *v*/*v*) was added and BTIC was precipitated and collected as a red solid (161.2 mg, 92%). ^{1}H NMR (400 MHz, $CDCl_3$) δ

8.87 (s, 1H), 8.00 (d, J = 8.1 Hz, 1H), 7.92 (d, J = 7.6 Hz, 1H), 7.50 – 7.42 (m, 2H), 7.37 – 7.31 (m, 1H), 6.63 (d, J = 11.4 Hz, 1H), 6.52 (d, J = 2.3 Hz, 1H), 3.45-3.40 (m, 4H), 2.60 (s, 1H), 1.24-1.21 (m, 6H). ^{13}C NMR (100 MHz, $CDCl_3$), δ 161.80, 161.06, 157.03, 152.57, 152.10, 142.03, 136.26, 130.77, 126.06, 124.42, 122.12, 121.56, 112.40, 109.98, 108.67, 96.97, 45.07, 40.96, 12.48. HRMS (MALDI-TOF): m/z: $[M+H]^+$ calcd for $C_{20}H_{20}N_3OS^+$: 350.1327; found: 350.1321.

Figures and tables:

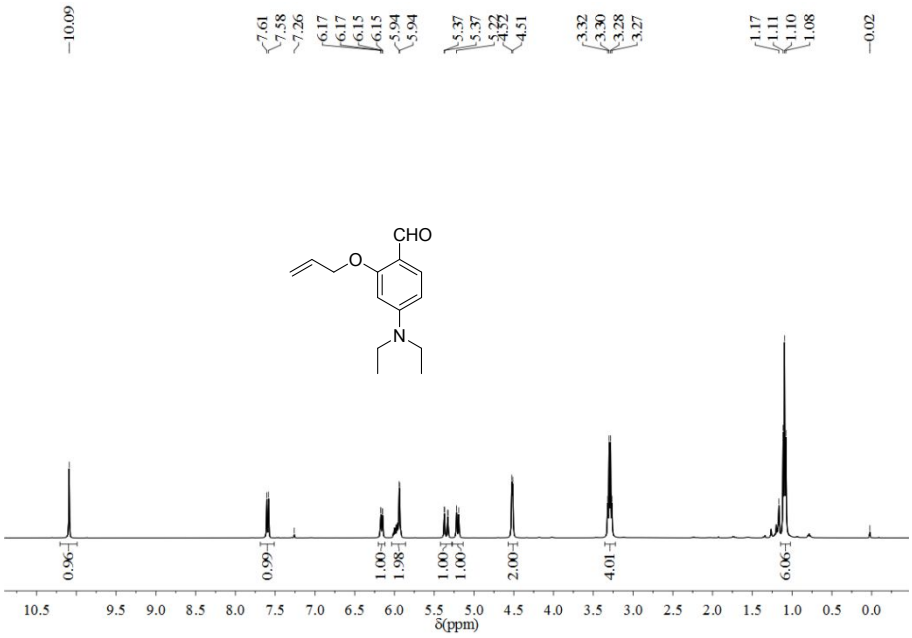

Figure S1. ^{1}H NMR spectrum of compound **3** in $CDCl_3$.

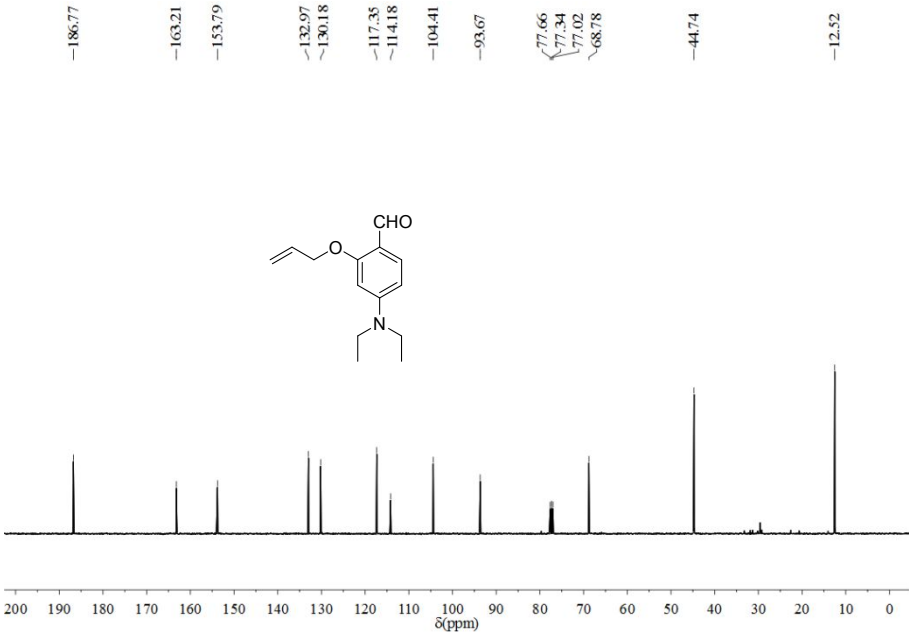

Figure S2. ^{13}C NMR spectrum of compound **3** in $CDCl_3$.

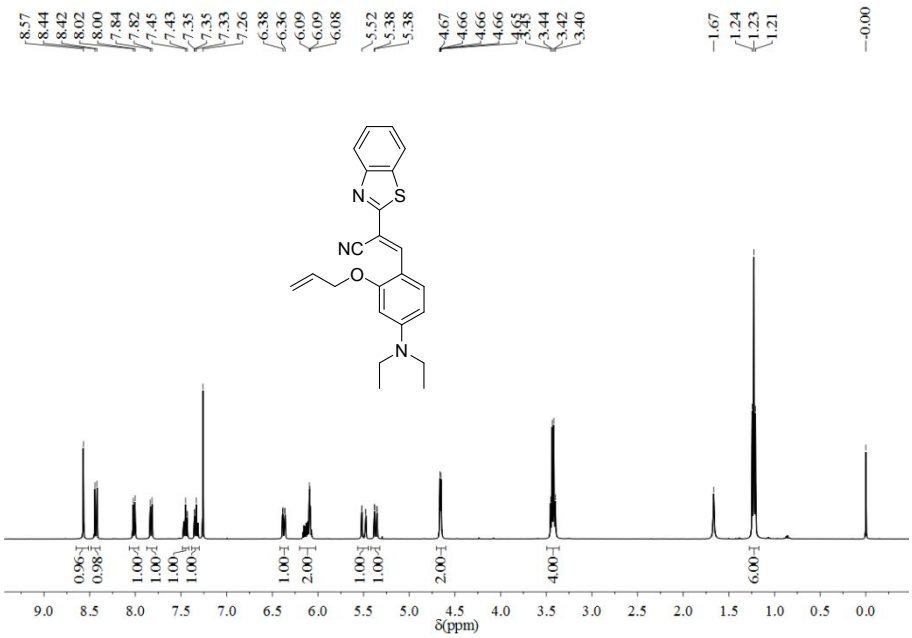

Figure S3. ^{1}H NMR spectrum of BTCV-CO in $CDCl_3$.

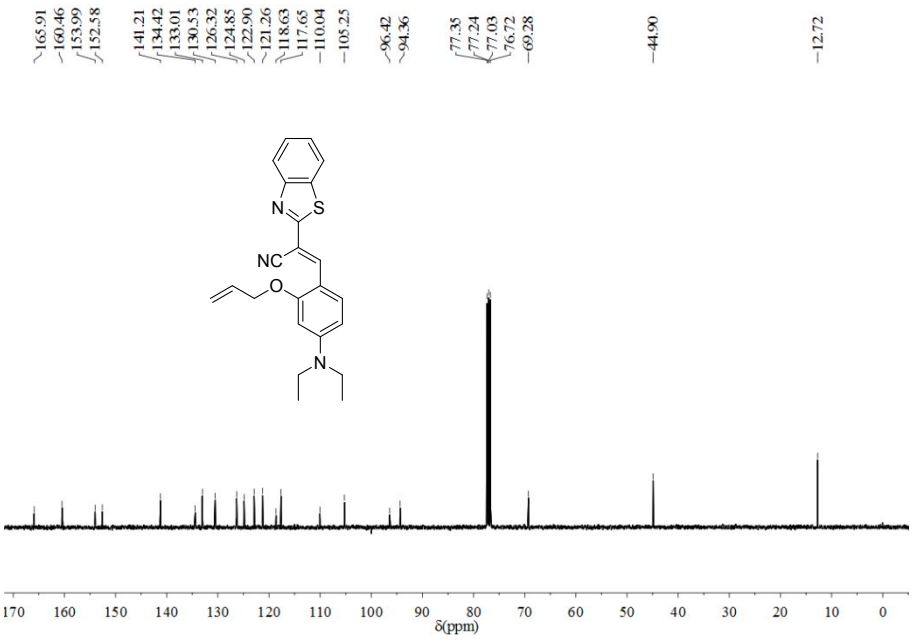

Figure S4. ^{13}C NMR spectrum of BTCV-CO in $CDCl_3$.

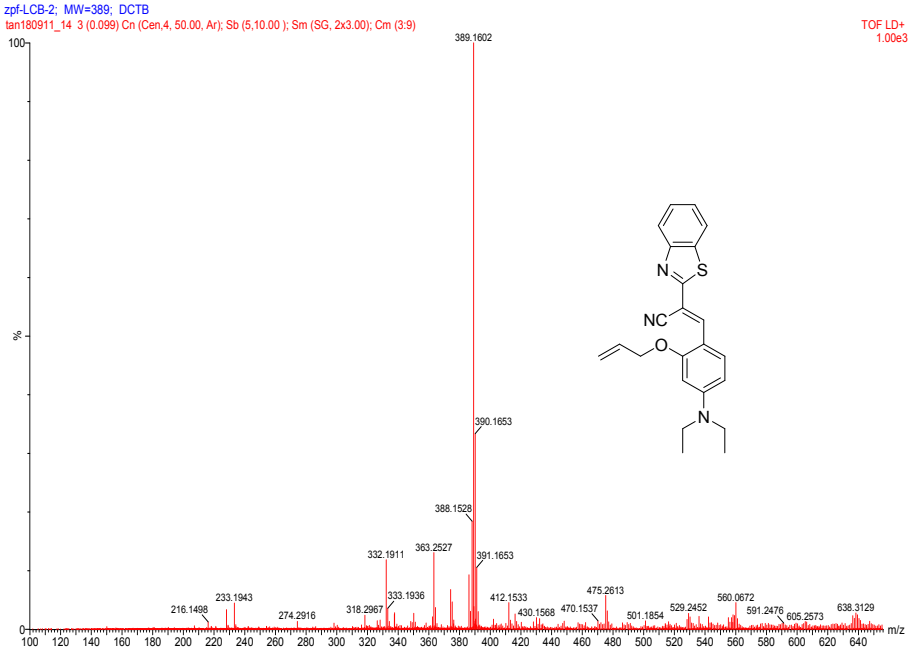

Figure S5. HRMS spectrum of BTCV-CO.

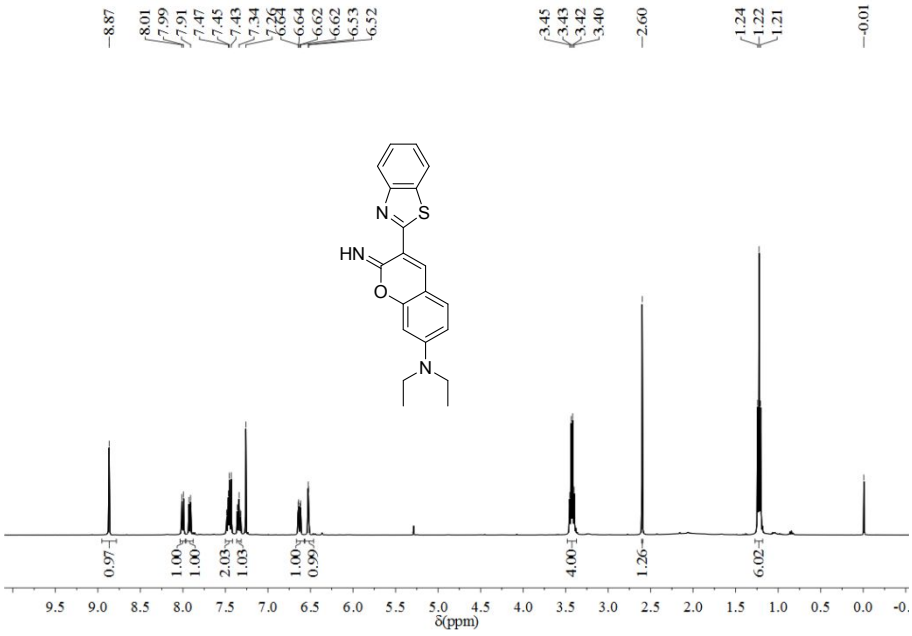

Figure S6. ^{1}H NMR spectrum of BTIC in $CDCl_3$.

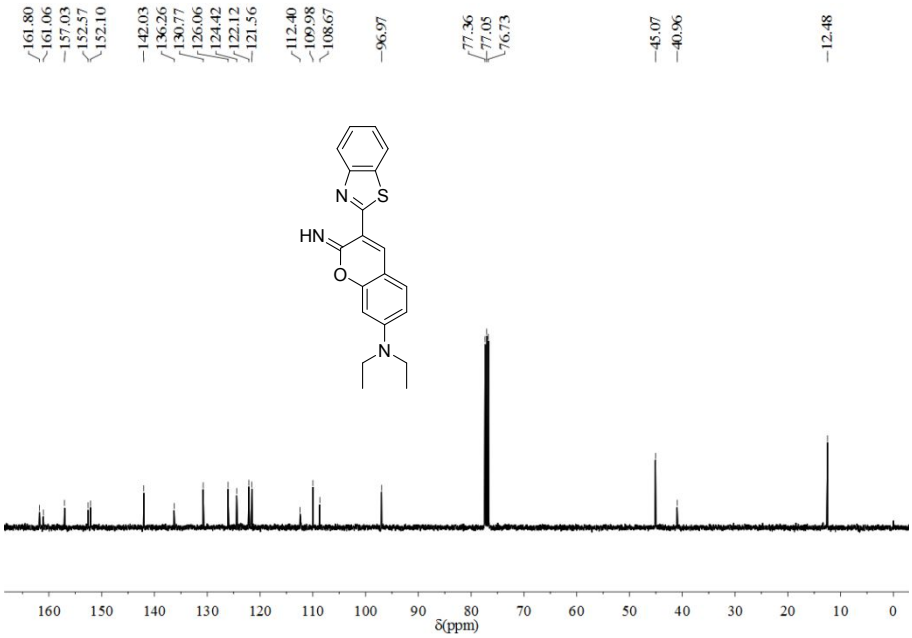

Figure S7. ^{13}C NMR spectrum of BTIC in $CDCl_3$.

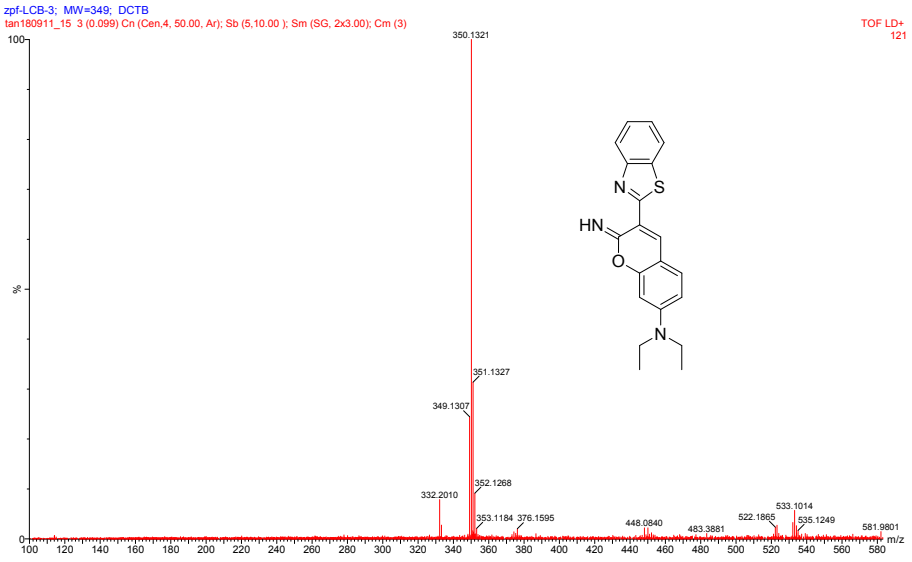

Figure S8. HRMS spectrum of BTIC.

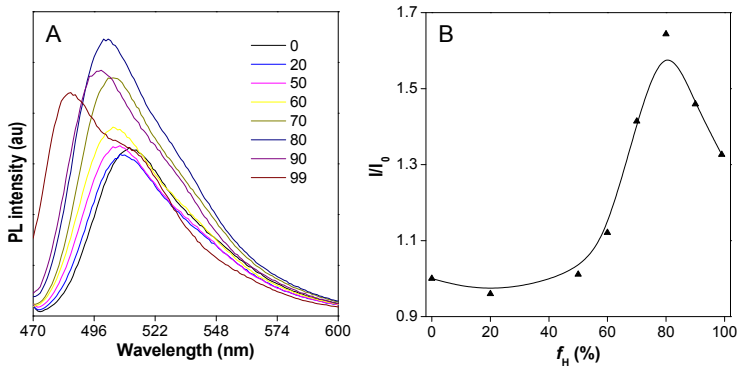

Figure S9. (A) PL spectra of BTIC in toluene/DMSO mixtures with different toluene fractions (f_H). (B) Plot of PL intensity of BTIC at maximum emission wavelength *vs*. f_H in the toluene/DMSO mixtures.

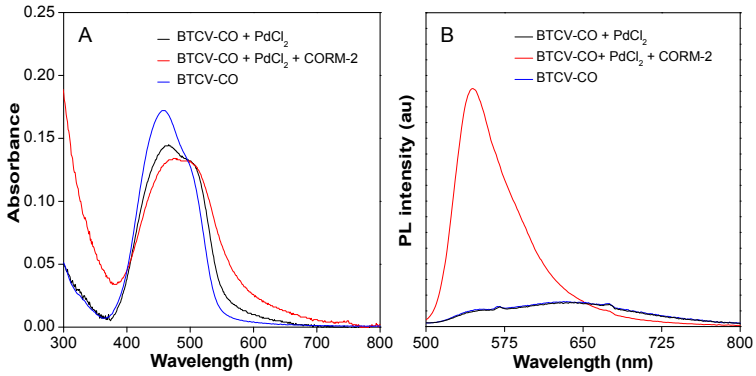

Figure S10. (A) UV/Vis spectra and (B) PL spectra of BTCV-CO (5 μM), BTCV-CO + $PdCl_2$ (5 μM) and BTCV-CO + $PdCl_2$ + CORM-2 (50 μM) at 37 °C for 20 min in 5% DMSO/PBS solution. Excitation wavelength (λ_{ex}) = 465 nm.

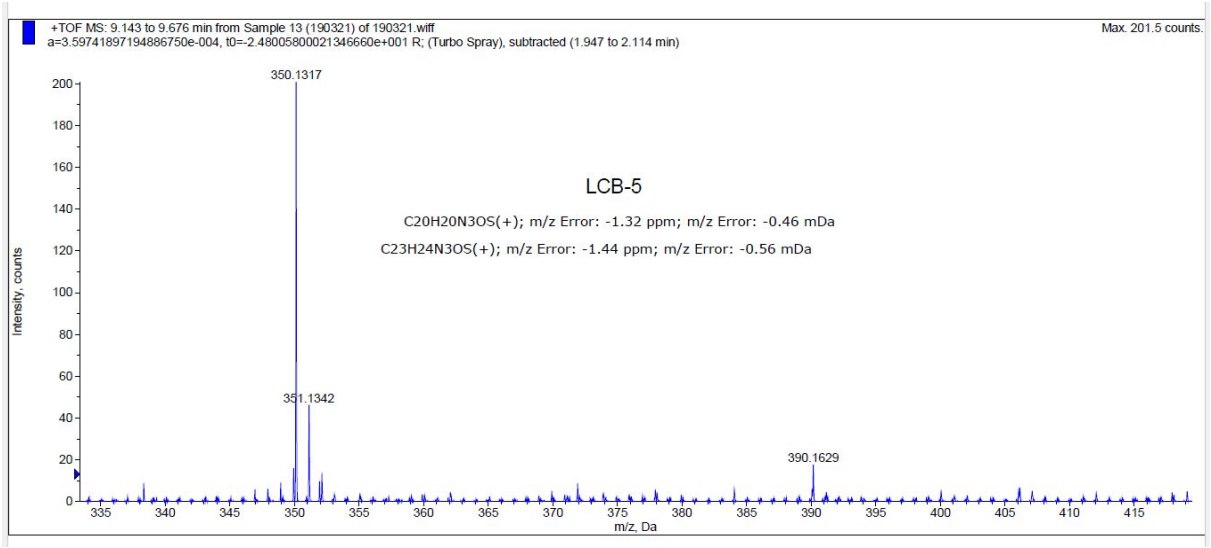

Figure S11. HRMS spectrum of BTCV-CO after incubation with $PdCl_2$ and CORM-2 (125 μM) at 37 °C for 20 min.

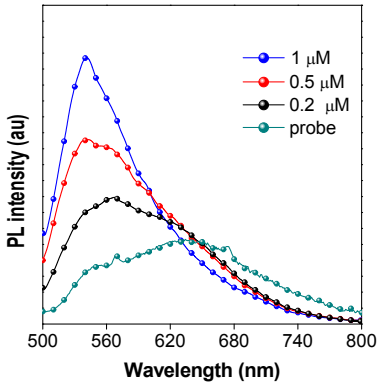

Figure S12. PL spectra of BTCV-CO (5 μM in PBS solution, pH 7.4, containing 5% DMSO) after incubation with CORM-2 (125 μM) in presence of $PdCl_2$ with different concentrations for 20 min.

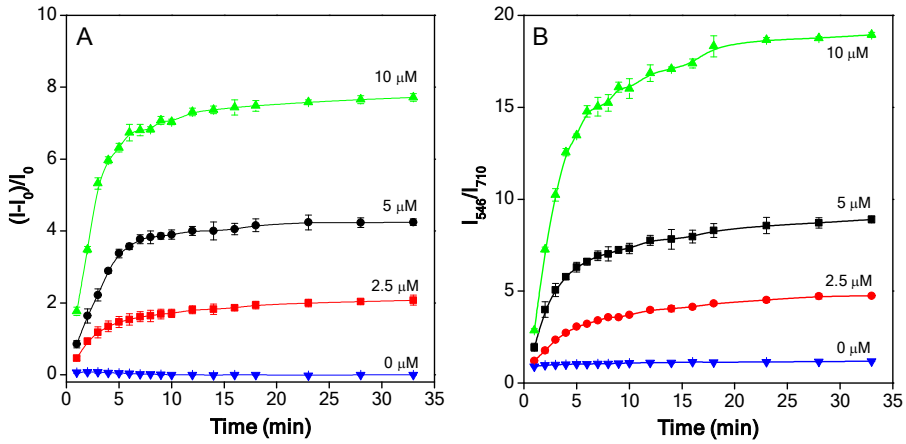

Figure S13. (A) The PL intensity ratios ($(I-I_0)/I_0$) of BTCV-CO (5 μM) + $PdCl_2$ (5 μM) at 546 nm in the presence of different concentrations of CORM-2 as a function of incubation time. (B) PL internsity ratios (I_{546}/I_{710}) of BTCV-CO (5 μM) + $PdCl_2$ (5 μM) in the presence of different concentrations of CORM-2 as a function of incubation time. λ_{ex} = 465 nm.

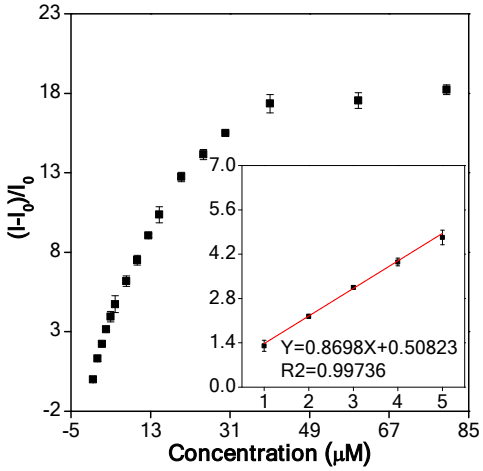

Figure S14.The PL intensity ratios ($(I-I_0)/I_0$) of BTCV-CO (5 μM) + $PdCl_2$ (5 μM) at 546 nm as a function of the concentration of CORM-2. Inset shows the linear relationship of the PL intensity ratios (I_{546}/I_{710}) as a function of the concentration of CORM-2. λ_{ex} = 465 nm.

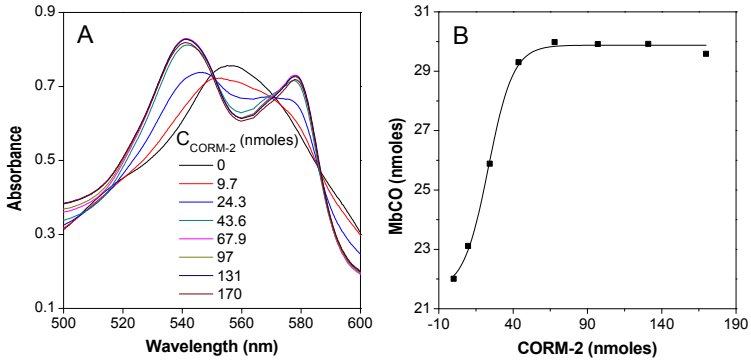

Figure S15. (A) Absorption spectrum of deoxy-Mb and MbCO before and after interaction of myoglobin with the different concentrations of CORM-2. (B) Determination of the amount of MbCO formed after interaction of deoxy-Mb with various concentrations of CORM-2.

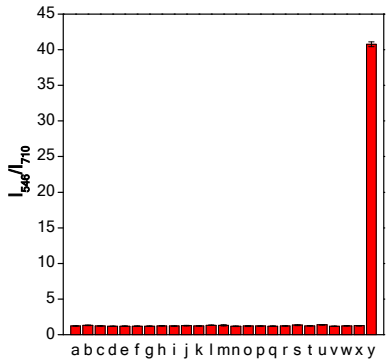

Figure S16.Variations of PL intensity ratios (I_{546}/I_{710}) of BTCV-CO (5 μM) + $PdCl_2$ (5 μM) after incubation with 100 μM CORM-2 or other biologically-relevant species. a: AcO^-; b: ClO^-; c: Glu; d: Cys; e: GSH; f: H_2O_2; g: H_2S; h: Hcy; i: HNO; j: Ile; k: Leu; l: Trp; m: Br^-; n: Cl^-; o: F^-; p: HCO_3^-; q: NO_2^-; r: ·OH; s: $ONOO^-$; t: $PdCl_2$; u: Phe; v: $ROO^·$; w: Ser; x: SO_4^{2-}; y: CORM-2. λ_{ex} = 465 nm.

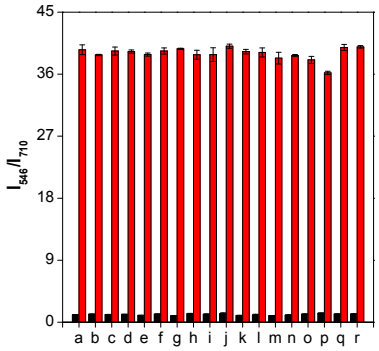

Figure S17. Variations of PL intensity ratios (I_{546}/I_{710}) of BTCV-CO + $PdCl_2$ (black bars) and BTCV-CO + $PdCl_2$ + CORM-2 (red bars) after incubation with 100 μM other biologically-relevant species. a: AcO^-; b: Glu c:Cys; d:GSH; e:H_2S; f: Hcy; g: Ile; h: Leu; i: Trp; j: Br^-; k: Cl^-; l: F^-; m: HCO_3^-; n: NO_2^-; o: $PdCl_2$; p: Phe; q: Ser; r: SO_4^{2-}. Concentrations: BTCV-CO and $PdCl_2$: 5 μM; CORM-2: 100 μM. λ_{ex} = 465 nm..

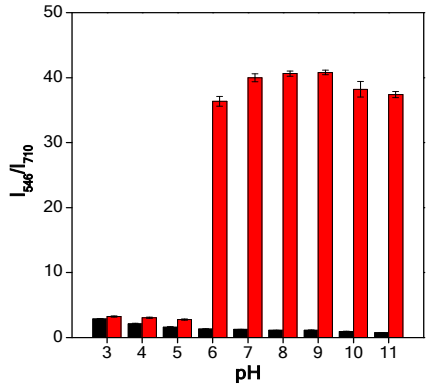

Figure S18.The PL intensity ratios (I_{546}/I_{710}) of BTCV-CO (5 μM, black bars) and BTCV-CO (5 μM) + $PdCl_2$ (5 μM) + CORM-2 (100 μM, red bars) in different pH buffers. λ_{ex} = 465 nm.

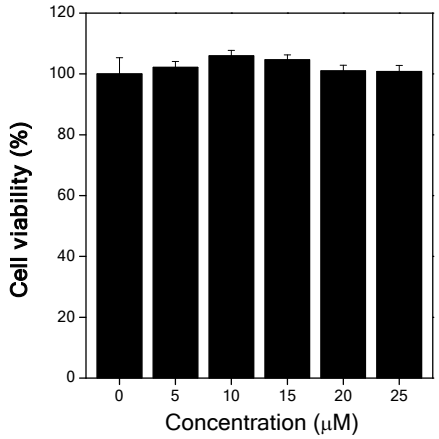

Figure S19. Cell viability of MCF-7 cells at varied concentrations of BTCV-CO by using standard MTT method.

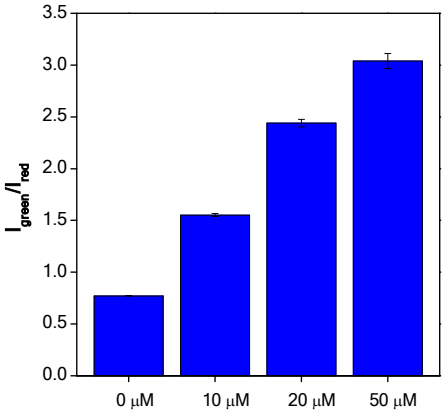

Figure S20. The PL intensity ratios (I_{green}/I_{red}) of the green channel and red channel in Figure 3.

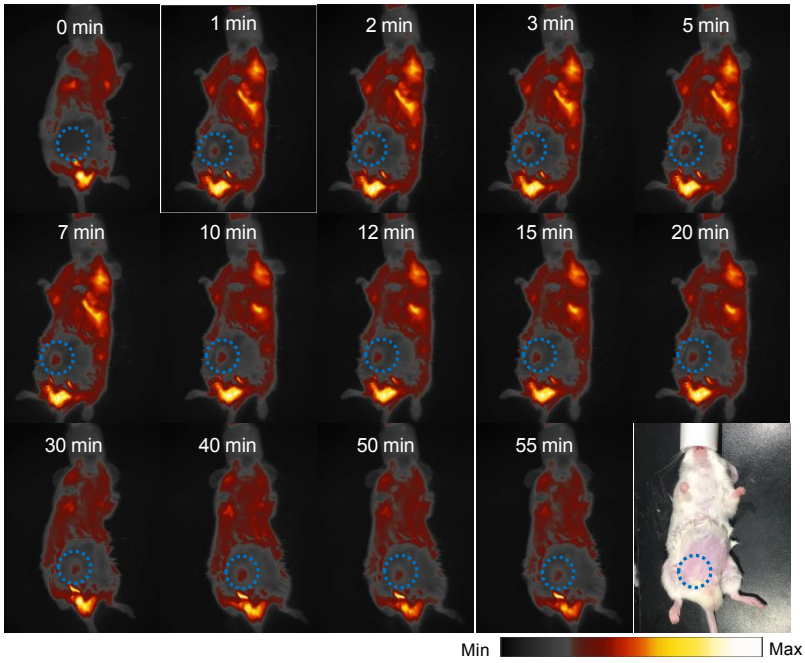

Figure S21. Time-dependent fluorescent images in live mice using probe BTCV-CO. BTCV-CO (20 nM) and $PdCl_2$ (20 nM) was injected in an intraperitoneal manner, followed by an injection of PBS (30 μL). Fluorescent emissions were collected from 580 to 700 nm. λ_{ex} = 523 nm.

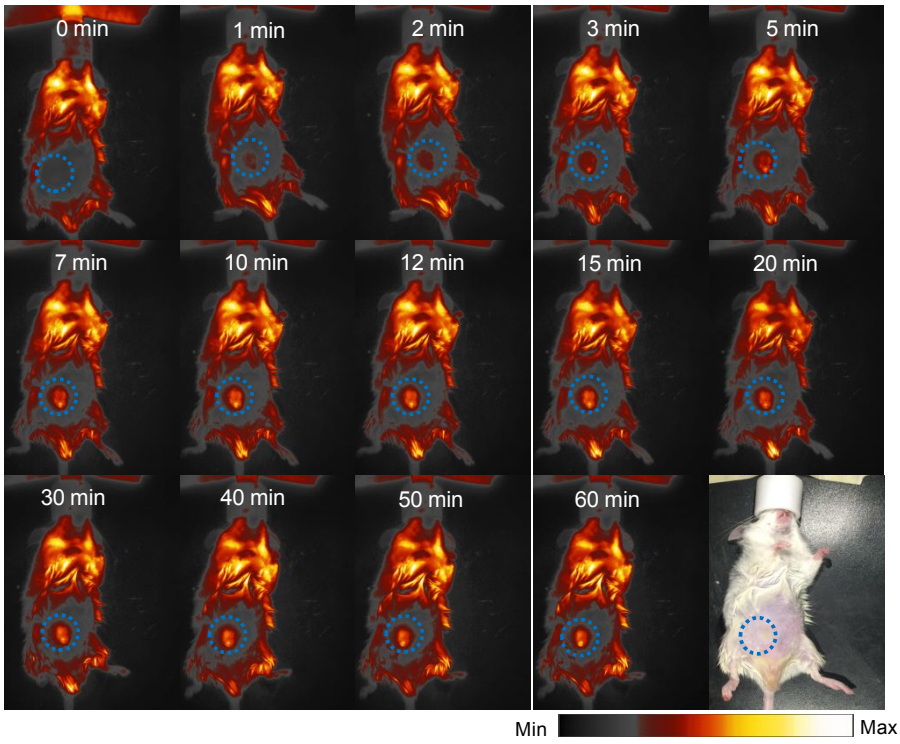

Figure S22. Time-dependent fluorescent images of CO in live mice using probe BTCV-CO. BTCV-CO (20 nM) and $PdCl_2$ (20 nM) was injected, followed by an injection of CORM-2 (150 nM). Fluorescent emissions were collected from 580 to 700 nm. λ_{ex} = 523 nm.

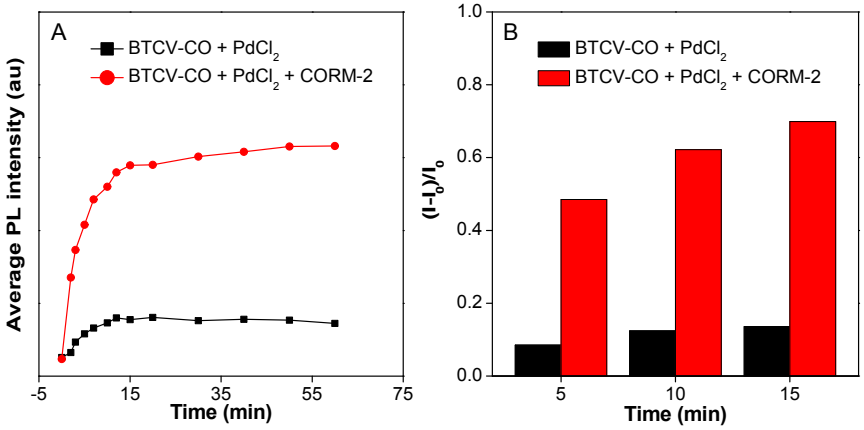

Figure S23. Time-dependent changes of average PL intensity (A) and PL intensity ratio ($(I-I_0)/I_0$) (B) in Figure S18 and S19.

Table S1. Comparison of some fluorescent probes for CO detection.

References	Response mode	Response time	Detection limit	λ_{em}	Imaging application
Angew. Chem. Int. Ed. 51 (2012) 9652	Turn-on (ACQ)	10 min	0.5 μM	528	cell
J. Am. Chem. Soc. 134 (2012) 15668	Turn-on (ACQ)	60 min	1 μM	507	cell
Chem. Sci. 5 (2014) 3439	Turn-on (ACQ)	40 min	0.653 μM	477	cell/tissue
Chem. Commun. 51 (2015) 4410	Turn-on (ACQ)	30 min	8.49 nM	450	cell
Tetrahedron Lett. 26 (2016) 2927	Turn-on (ACQ)	30 min	26.3 nM	549	cell
RSC Adv. 6 (2016) 65373	Turn-on (ACQ)	45 min	0.127 μM	670	cell
Anal. Chem. 88 (2016) 11154	Turn-on (ACQ)	30 min	0.72 μM	512	cell
Anal. Chem. 88 (2016) 10648	Turn-on (ACQ)	15 min	37 nM	520	cell
Anal. Chem. 89 (2017) 3754	Turn-on (ACQ)	20 min	**1:** 46 nM **2:** 29 nM	**1:** 516 **2:** 527	cell
Sens. Actuators B Chem. 240 (2017) 625	Turn-on (ACQ)	15 min	25 nM	496	cell
J. Am. Chem. Soc. 139 (2017) 18484	Turn-on (ACQ)	ND	ND	450	cell/*ex vivo*
Angew. Chem. Int. Ed. 56 (2017) 13489	Turn-on (ACQ)	30 min	0.5 nM	660	cell/zebrafish/tissue/ organ/mice
Anal. Chem. 90 (2018) 2933	Turn-on (ACQ)	45 min	0.6 μM	525	cell
ACS sens. 3 (2018) 285	Turn-on (ACQ)	20 min	0.06 μM	415	cell
Spectrochim. Acta A 202 (2018) 284	Turn-on (ACQ)	40 min	57 nM	685	cell
Talanta 188 (2018) 691	Turn-on (ACQ)	18 min	0.17 μM	736	cell/tissue/mice
Sens. Actuators B Chem. 255 (2018) 2314	Turn-on (ACQ)	3 min	3.2 nM	714	cell/mice
New J. Chem. 42 (2018) 13497	Turn-on (ACQ)	45 min	123 nM	520	cell
Anal. Chem. 90 (2018) 7117	Turn-on (ACQ)	40 min	0.18 μM	550	cell/zebrafish
Anal. Methods, 11 (2019) 288	Turn-on (ACQ)	20 min	38.9 nM	630	cell
Chem. Sci. 10 (2019) 320	Turn-on (ACQ)	30 min	0.23 μM	650	cell/tissue/mice
Chem. Eur. J. 25 (2019) 2069	Turn-on (ACQ)	ND	ND	450	cell
Sens. Actuators B Chem. 291 (2019) 329	Turn-on (ACQ)	10 min	6.1 nM	665	cell/ zebrafish
Sens. Actuators B Chem. 251 (2017) 389	Ratiometric (ACQ)	20 min	58 nM	472/545	cell
New J. Chem. 42 (2018) 14417	Ratiometric (ACQ)	25 min	17.9 nM	545/455	cell
Anal. Chem. 91 (2019) 2939	Ratiometric (ACQ)	60 min	0.44 μM	540/610	cell/tissue/*D. magna*
This work	**Ratiometric (AIE)**	**20 min**	**30.8 nM**	**564/710**	**cell/mice**

References:

(S1) Beckman, J. S.; Chen, J.; Ischiropoulos, H.; Crow, J. P. *Method. Enzymol.* **1994**, *233*, 229-240.